Nuclear Engineering and Technology 52 (2020) 2543–2551

Contents lists available at ScienceDirect

Nuclear Engineering and Technology

journal homepage: www.elsevier.com/locate/net

Original Article

Equilibrium calculations for HyBRID decontamination of magnetite: Effect of raw amount of $CuSO_4$ on Cu_2O formation

Byung-Chul Lee [a, *], Seon-Byeong Kim [b], Jei-Kwon Moon [b]

[a] Department of Chemical Engineering, Hannam University, 1646 Yuseong-daero, Yuseong-gu, Daejeon, South Korea
[b] Decommissioning Technology Research Division, Korea Atomic Energy Research Institute, 111 Daedeok-daero 989 Beon-gil, Yuseong-gu, Daejeon, South Korea

ARTICLE INFO

Article history:
Received 18 December 2019
Received in revised form
7 April 2020
Accepted 9 April 2020
Available online 17 April 2020

Keywords:
HyBRID decontamination
Reductive dissolution
Equilibrium calculations
Magnetite
Aqueous solution model

ABSTRACT

Calculations of chemical equilibrium for multicomponent aqueous systems of the HyBRID dissolution of magnetite were performed by using the HSC Chemistry. They were done by using a Pitzer-based aqueous solution model with the recipe of raw materials in experiments conducted at KAERI. The change in the amounts of species and ions and the pH values of the solution at equilibrium was observed as functions of temperature and raw amount of $CuSO_4$. Precipitation of Cu_2O occurred at a large amount of $CuSO_4$ added to the solution, while no precipitation of $Cu(OH)_2$ was found at any amounts of $CuSO_4$. The E-pH diagrams for Cu were constructed at various Cu concentrations to provide the effect of the Cu concentration on the pH values at boundaries where the coexistence of Cu^+ ion and Cu_2O solid occurred. To prevent Cu^+ ions from being precipitated to Cu_2O, the raw amount of $CuSO_4$ should be adjusted so that the pH value of the solution from the equilibrium calculation is less than that from the E-pH diagram. We provided guidelines for the raw amount of $CuSO_4$ and the pH value of the solution, which prevent the formation of Cu_2O precipitates in the HyBRID dissolution experiments for magnetite.

1. Introduction

Structural alloy materials used in the coolant system of a nuclear power plant (NPP) are mostly composed of iron-based low alloy steel and stainless steel, nickel-based Inconel, and zirconium-based Zircaloy. The spinel-type transition metal oxides such as magnetite, nickel ferrite and chromite are deposited on the surface of structures like pipes and equipments, especially when in contact with the coolant. Decontamination is conducted for equipment and systems which have been contaminated by the activity build-up with time evolution for a reduction of occupational exposure during maintenance or decommissioning, and additionally on depleting the radioactive waste at the time for decommissioning. Especially, the primary coolant system of the NPP gets deposited with radionuclides (e.g. Co-60) after long-term operation. The removal of the radionuclides from the primary coolant system takes place with the dissolution of corrosion metal oxide layers deposited with the radionuclides [1]. The dissolution of the corrosion metal oxide up to the boundary layer of the oxide and the base metal is required to remove all the radioactive species from the target surface.

Chemical decontamination by oxidative and reductive dissolution is considered to be the most effective method to date. The reductive decontamination processes such as CAN-DEREM, CITROX, LOMI, and CORD to dissolve the iron oxides have been widely used in the decontamination of the NPP primary coolant system. Acidic solutions such as oxalic acid, citric acid, ethylenediaminetetraacetic acid (EDTA), and their mixtures are used as reducing agents [2]. In most commercial reductive decontamination processes, organic chelates are used to prevent the precipitation of dissolved metal ions by forming metal-organic acid chelation. The use of organic chelates results in improved decontamination efficiency. However, it was found that the organic acids and chelates used in those processes gave detrimental effects for disposal safety due to the formation of stable and soluble complexes with radionuclides [3]. There is also a risk of potential release of chemo-toxic substances in the event of an accident in the final repository [1]. KAERI has developed a chemical decontamination process called “HyBRID” (Hydrazine Based Reductive metal Ion Decontamination) process that does not use organic acids or organic chelating agents at all [4–8].

* Corresponding author.
E-mail address: bclee@hnu.kr (B.-C. Lee).

https://doi.org/10.1016/j.net.2020.04.012

In the HyBRID process, the solution containing sulfuric acid (H_2SO_4), hydrazine (N_2H_4), and copper sulfate ($CuSO_4$) provided the acidic and reductive dissolution of transition metal ions from the corrosion metal oxides like magnetite (Fe_3O_4). In our previous publication [9], we proposed the plausible mechanisms of the dissolution reactions involved in the HyBRID process for corrosion metal oxides. Complete sets of dissolution reactions were made for the metal oxides, and then the reaction spontaneity was evaluated by comparing the equilibrium constants as a function of temperature for the individual reactions.

In this work we tried to provide the thermodynamic characteristics of the proposed reactions. Traditional researches in thermodynamic calculations have been based on experimental or assessed data contained in scientific journals, but searching for necessary data from vast references is limited and time-consuming. We aimed the HyBRID chemical decontamination process to be plausible using thermochemical calculations from a thermodynamic point of view. Since the HyBRID decontamination process does not use any organic chelates, precipitates of metal ions can be formed as the solution pH changes. Under a reducing condition, Cu^+ ions may form precipitates of Cu_2O or be hydrolyzed into $Cu(OH)_2$ precipitates. Pathways of the hydrolysis of the Cu^+ ions will be discussed as well. Thus it is important to find the reducing conditions at which no precipitation of Cu_2O or $Cu(OH)_2$ is formed. In this work we studied the effect of the concentration of copper ions in the HyBRID aqueous solution on the formation of Cu_2O or $Cu(OH)_2$ precipitates for the HyBRID dissolution of magnetite. Raw amount of $CuSO_4$ was changed in order to control the concentration of copper ions. The possibility of the formation of precipitates of metal ions (e.g. Cu_2O) during the decontamination was investigated.

2. Reaction scheme and calculation methods

The HyBRID chemical decontamination for the primary coolant system consists of the acidic dissolution by an acid and the reductive dissolution by a reducing agent in order to dissolve transition metal ions from the corrosion metal oxides deposited on the surface of the coolant system. Hydrazine is used as a strong reducing agent and copper ion is used as a catalyst to form copper-hydrazine complexes which transfer electrons from a cuprous ion (Cu^+) to a ferric ion (Fe^{3+}) to be reduced to a ferrous ion (Fe^{2+}) [6]. Sulfuric acid is used to control the pH of the solution.

The dissolution mechanism in the HyBRID decontamination is very complex because of the presence of hydrazine, which acts as a reducing agent, and a Cu^{2+}/Cu^+ ion pair, which acts as a redox couple. Through our previous studies [6–8, 10], Cu^{2+} ions were observed to be reduced by hydrazine to produce Cu^+ ions. The resulting Cu^+ ions were oxidized to Cu^{2+} ions after reducing the Fe_3O_4 layer, and the Cu^{2+} ions were then rapidly reduced to Cu^+ ions by hydrazine, thereby completing redox cycling. Consequently, hydrazine contributes both to acidic dissolution and to reductive dissolution by providing hydrogen ions and electrons in solution. It participates in the reaction pathway of reducing Fe^{3+} ions to Fe^{2+} ions and simultaneously regenerating oxidized Cu^{2+} ions into Cu^+ ions, as shown schematically in Fig. 1 [10]. During the cycle of Cu^+ ions to Cu^{2+} ions, the released electrons promote the reduction of Fe^{3+} ions.

Additionally, the dissolution of Fe_3O_4 by addition of hydrazine and copper ions can be discussed in terms of kinetics for redox reactions. From the previous study [10], it is clear that copper ions after being dissolved from $CuSO_4$ must exist in the form of Cu^+ by the reducing conditions formulated by hydrazine and the dissolution of Fe_3O_4 is also facilitated by the reduction of Fe^{3+} to Fe^{2+}. The results of kinetics showed the dissolution rate increased by the addition of hydrazine and copper ions, indicating that the reducing power increased by hydrazine as well as copper ions.

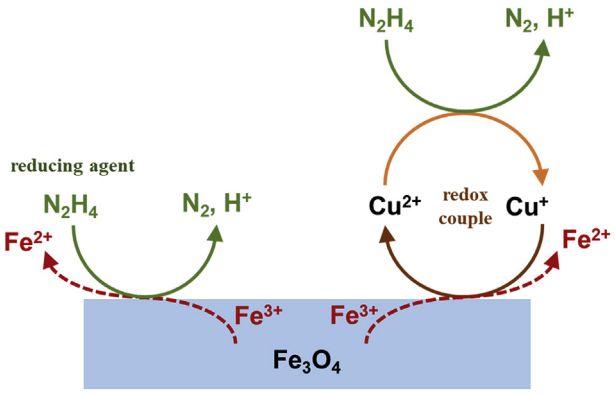

Fig. 1. A schematic diagram of the dissolution mechanism of magnetite in the HyBRID decontamination.

2.1. Reaction mechanism of HyBRID dissolution of magnetite

The dissolution reactions of magnetite in aqueous solution of sulfuric acid is:

$$Fe_3O_4 + H_2SO_4 \rightarrow Fe^{2+} + Fe_2O_3 + SO_4^{2-} + H_2O \quad (R1)$$

$$Fe_2O_3 + 3H_2SO_4 \rightarrow 2Fe^{3+} + 3SO_4^{2-} + 3H_2O \quad (R2)$$

$$Fe_3O_4 + 4H_2SO_4 \rightarrow Fe^{2+} + 2Fe^{3+} + 4SO_4^{2-} + 4H_2O \quad (R3)$$

When liquid hydrazine (N_2H_4) is added to the solution, it is readily protonated to produce hydrazinium ions ($N_2H_5^+$) by the reaction:

$$N_2H_4 + H^+ \rightarrow N_2H_5^+ \quad (R4)$$

Fe^{3+} ions are reduced to Fe^{2+} by $N_2H_5^+$:

$$2Fe^{3+} + \frac{1}{2}N_2H_5^+ \rightarrow 2Fe^{2+} + \frac{1}{2}N_2 + \frac{5}{2}H^+ \quad (R5)$$

Combining reactions (R4) and (R5) gives

$$2Fe^{3+} + \frac{1}{2}N_2H_4 \rightarrow 2Fe^{2+} + \frac{1}{2}N_2 + 2H^+ \quad (R6)$$

Therefore, the following reaction is obtained by combining reactions (R3) and (R6):

$$Fe_3O_4 + \frac{1}{2}N_2H_4 + 4H_2SO_4 \rightarrow 3Fe^{2+} + 4SO_4^{2-} + \frac{1}{2}N_2 + 2H^+ + 4H_2O \quad (R7)$$

$CuSO_4$ dissociates as soon as it is added to the aqueous solution:

$$CuSO_4 \leftrightarrow Cu^{2+} + SO_4^{2-} \quad (R8)$$

Cu^{2+} ions are reduced to the Cu^+ ions by the reaction with $N_2H_5^+$:

$$2Cu^{2+} + \frac{1}{2}N_2H_5^+ \leftrightarrow 2Cu^+ + \frac{1}{2}N_2 + \frac{5}{2}H^+ \quad (R9)$$

From reactions (R4), (R8) and (R9), the following reactions can be obtained:

$$2CuSO_4 + \frac{1}{2}N_2H_5^+ \leftrightarrow 2Cu^+ + 2SO_4^{2-} + \frac{1}{2}N_2 + \frac{5}{2}H^+ \quad (R10)$$

$$2CuSO_4 + \frac{1}{2}N_2H_4 \leftrightarrow 2Cu^+ + 2SO_4^{2-} + \frac{1}{2}N_2 + 2H^+ \quad (R11)$$

Reduction of Fe^{3+} to Fe^{2+} by oxidative regeneration of Cu^+ to Cu^{2+} is

$$Fe^{3+} + Cu^+ \rightarrow Fe^{2+} + Cu^{2+} \quad (R12)$$

Reactions (R3) and (R12) are combined to yield

$$Fe_3O_4 + 2Cu^+ + 4H_2SO_4 \rightarrow 3Fe^{2+} + 2Cu^{2+} + 4SO_4^{2-} + 4H_2O \quad (R13)$$

Hydrazine facilitates the transfer of electrons to Fe^{3+} in magnetite via Cu^{n+} ions. Finally, from reactions (R10) and (R13), the dissolution reaction of magnetite can be summarized as follows:

$$Fe_3O_4 + 2CuSO_4 + \frac{1}{2}N_2H_5^+ + 4H_2SO_4 \rightarrow 3Fe^{2+} + 2Cu^{2+} + 6SO_4^{2-} + \frac{1}{2}N_2 + \frac{5}{2}H^+ + 4H_2O \quad (R14)$$

Similarly, combining reactions (R11) and (R13) gives

$$Fe_3O_4 + 2CuSO_4 + \frac{1}{2}N_2H_4 + 4H_2SO_4 \rightarrow 3Fe^{2+} + 2Cu^{2+} + 6SO_4^{2-} + \frac{1}{2}N_2 + 2H^+ + 4H_2O \quad (R15)$$

Considering the chemical reaction scheme in which HSO_4^- anions are formed instead of SO_4^{2-} anions when H_2SO_4 dissociates, the main dissolution reactions for magnetite can be expressed as follows:

$$Fe_3O_4 + 5H_2SO_4 \leftrightarrow Fe^{2+} + 2Fe^{3+} + 5HSO_4^- + 3OH^- + H_2O \quad (R16)$$

$$Fe_3O_4 + \frac{1}{2}N_2H_4 + 5H_2SO_4 \leftrightarrow 3Fe^{2+} + 5HSO_4^- + \frac{1}{2}N_2 + 2H^+ + 3OH^- + H_2O \quad (R17)$$

$$Fe_3O_4 + 2CuSO_4 + \frac{1}{2}N_2H_4 + 5H_2SO_4 \leftrightarrow 3Fe^{2+} + 2Cu^{2+} + 2SO_4^{2-} + 5HSO_4^- + \frac{1}{2}N_2 + 2H^+ + 3OH^- + H_2O \quad (R18)$$

2.2. Method of equilibrium calculations

The theory of calculating multiphase equilibria at fixed temperature and pressure is based on the Gibbs free energy minimization principle [11–13]. The solution to the following minimization problem is required.

Minimize

$$G^t = \sum_{i=1}^{N} n_i \mu_i \quad (1)$$

subject to

$$\sum_{i=1}^{N} n_i c_{ij} = b_j, \quad j = 1, M + P_E \quad (2)$$

$$n_i \geq 0, \quad i = 1, N \quad (3)$$

In these equations, G^t is the total Gibbs free energy for the system; n_i is the number of moles of species i; μ_i is the chemical potential for species i; b_j is the number of moles of component j; c_{ij} are the coefficients in the linear mass and charge balance equations; N is the total number of species; P_E is the number of possible electrolyte aqueous and solid solution phases; and M is the total number of components.

It is conventional to define the activities of the species, a_i, in electrolyte solutions by the following equation [14–17]:

$$\left(\frac{\partial G^t}{\partial n_i}\right)_{T,P,n_{j\neq i}} = \mu_i = \mu_i^0 + RT \ln a_i \quad (4)$$

where μ_i^0 is the standard chemical potential for species i. The activity and osmotic coefficients are defined by

$$\ln a_i = \ln(\gamma_i m_i) \quad (5)$$

for each solute species i and

$$\ln a_w = -\frac{W}{1000}\left(\sum_i m_i\right)\phi \quad (6)$$

for the solvent (water). γ_i and m_i are the activity coefficient and molality of the solute species i. The osmotic coefficient, ϕ, is related to the activity of water by Eq. (6) where W is the molecular mass of water. The sum over i in Eq. (6) represents the sum over all solutes: cations, anions and neutrals.

The chemical potentials for pure phases, such as minerals, are constant at a fixed temperature and pressure. For gases, the fugacity of a gas phase species, f_i, is defined by

$$\mu_i = \mu_i^0 + RT \ln f_i \quad (7)$$

For many gases below or near 1 bar, the fugacity nearly equals the partial pressure, P_i.

Ionic systems deviate from ideality even in very dilute solutions, due to significant long-range electrostatic forces between ions. Thus, electrolyte solutions are non-ideal even at low solute concentrations. Adequate thermodynamic models are necessary for the determination of the properties of aqueous electrolyte systems. For practical applications, it is still necessary to rely on semi-empirical models. One of the most widely used semi-empirical models was developed by Pitzer [11] and later modified by Harvie et al. [12]. The Pitzer equations form a quite solid and theoretically realistic foundation for the calculation of aqueous system thermodynamics. The Pitzer model is usually valid up to 6 molality. Therefore, it is well suited to apply the Pitzer model to our system based on 1 molality.

In this work, the Harvie's modification of the Pitzer model was used to model the excess functions: γ_i and $(\phi - 1)$. The model equations for calculating the activity coefficients of cations and anions in a multicomponent solution are expressed as follows [12]:

$$\ln \gamma_M = z_M^2 F + \sum_a m_a (2B_{Ma} + ZC_{Ma}) + \sum_c m_c \left(2\Phi_{Mc} + \sum_a m_a \Psi_{Mca} \right) + \sum_a \sum_{a'>a} m_a m_{a'} \Psi_{Maa'} + |z_M| \sum_c \sum_a m_c m_a C_{ca} + 2\sum_n m_n \lambda_{nM} \quad (8)$$

$$\ln \gamma_X = z_X^2 F + \sum_c m_c (2B_{cX} + ZC_{cX}) + \sum_a m_a \left(2\Phi_{Xa} + \sum_c m_c \Psi_{Xac} \right) + \sum_c \sum_{c'>c} m_c m_{c'} \Psi_{cc'X} + |z_X| \sum_c \sum_a m_c m_a C_{ca} + 2\sum_n m_n \lambda_{nX} \quad (9)$$

$$\ln \gamma_N = 2\sum_c m_c \lambda_{nc} + 2\sum_a m_a \lambda_{na} \quad (10)$$

where $Z = \sum m_i |z_i|$. m_c is the molality of cation, c, with charge z_c. The subscripts M, c and c' refer to cations, while the subscripts X, a and a' refer to anions. The subscripts N and n denote neutrals. The function F is the sum of the Debye-Hückel term and terms with derivatives of the second virial coefficients with respect to ionic strength. B's and Φ's represent measurable combinations of the second virial coefficients and depend on ionic strength. C's and Ψ's, assumed to be independent of ionic strength, are measurable combinations of the third virial coefficients. B's and C's are parameterized from single electrolyte data, while Φ's and Ψ's are parameterized from two salt systems. λ_{ni} are the second virial coefficients representing the interactions between ions and neutral species.

Another extremely essential property of the aqueous solution is the pH value of the solution, which is the 10-base logarithm of the hydrogen ion activity in the solution:

$$\mathrm{pH} = -\log_{10} a_{H^+} = -\log_{10} (\gamma_{H^+} m_{H^+}) \quad (11)$$

where γ_{H^+} is the molal activity coefficient of hydrogen ion and m_{H^+} is the molality of hydrogen ion.

Calculations of the multicomponent chemical equilibrium in a heterogeneous aqueous system like the HyBRID dissolution of magnetite were conducted using the GEM module of the HSC Chemistry® 9 [18]. When the initial amounts of raw species were given, the amounts and activity coefficients of ions and neutrals involved in the dissolution reactions at equilibrium were calculated at various temperatures using the GIBBS solver, which used the Gibbs energy minimization method. In addition, the pH values of the aqueous solution were also calculated. The equilibrium calculations were carried out in the temperature range from 25 °C to 95 °C. For a multicomponent aqueous solution, an aqueous solution model based on the Harvie's modification of the Pitzer model [12] was used to calculate activity coefficients of the aqueous species (neutral components, ionic species and water). Gas phase was assumed to behave as an ideal mixture. The Pitzer parameter database in the AQUA module, including temperature-dependent binary and ternary ion interaction parameters, were used for the multicomponent aqueous solutions [17]. The AQUA module was used for the estimation of ion activities, activity coefficients, osmotic coefficient of water, enthalpies, heat capacities, and pH values of homogeneous aqueous solutions.

2.3. Construction of E-pH diagram

To determine the effect of the concentration of copper ions in the HyBRID dissolution of magnetite, the E-pH (Pourbaix) diagram for Cu was first constructed and then compared with the equilibrium composition and pH of the solution. The E-pH diagram illustrates the thermodynamic stability areas of different species in an aqueous solution. Stability areas are presented as functions of pH and redox potential scales at a selected temperature and concentration. Thus, the E-pH diagram for Cu gives the stability areas where species and ions such as Cu^+, Cu^{2+}, Cu_2O, $Cu(OH)_2$ are present depending on the pH and the redox potential. The E-pH module in the HSC Chemistry® version 9 was used to construct the E-pH diagram for the Cu system. The module is based on STABCAL (Stability Calculations for Aqueous Systems) developed by Haung [19]. Temperature and pressure of the system were set to 95 °C and 1 bar, respectively.

3. Results and discussion

Table 1 shows the recipe of experiments conducted at KAERI for the HyBRID dissolution of magnetite. The equilibrium calculations were also performed at the same conditions as shown in Table 1. Raw amount of $CuSO_4$ was varied from 5.0E-04 to 1.0E-01 in mole to observe the effect of the raw amount of $CuSO_4$ on the chemical equilibrium, while raw amounts of Fe_3O_4, N_2H_4, H_2SO_4, and H_2O in the feed were kept constant. Equilibrium calculations were repeatedly performed at various amounts of raw $CuSO_4$, and the calculation results at two representative raw amounts of $CuSO_4$ (5.0E-04 mol and 5.0E-02 mol) are shown in Tables 2 and 3, respectively. Note that the raw amounts of all other species fed to the aqueous phase are the same. The equilibrium amounts and activity coefficients of species and ions are shown at 10 °C intervals in the temperature range from 25 °C to 95 °C. The pH values of the aqueous solution are also shown at the same temperatures.

The equilibrium amount of the Fe^{3+} ion was almost negligible at all temperatures, which can be attributed to the reduction of Fe^{3+} ions to Fe^{2+} ions by N_2H_4 as shown in the reaction scheme (R6). Similarly, the equilibrium amount of Cu^{2+} was negligibly small due to the reduction of Cu^{2+} to Cu^+ by the reaction with $N_2H_5^+$, as given in the reaction scheme (R9). This can also be demonstrated by the reduction of Fe^{3+} ions to Fe^{2+} ions by the oxidative regeneration of Cu^+ ions to Cu^{2+} ions, as shown in the reaction scheme (R12). As can be verified from the equilibrium amounts of N_2H_4 and $N_2H_5^+$, almost all of N_2H_4 fed into the aqueous solution was protonated to produce $N_2H_5^+$ ions by the reaction scheme (R4). According to the data of Tables 2 and 3, it can be seen that solid raw materials of Fe_3O_4, Fe_2O_3, and $CuSO_4$ fed to the aqueous phase were all dissolved, regardless of the amount of raw $CuSO_4$ added.

However, some interesting results have been observed as far as the precipitation of Cu_2O solids during the HyBRID decontamination is concerned. For a smaller amount of raw $CuSO_4$ (5.0E-04 mol), there was no Cu_2O solids precipitated from the aqueous solution. On

Table 1
Recipe of experiments conducted at KAERI for the HyBRID dissolution of magnetite.

Reagent	Phase	Raw amount [mol]
Fe_3O_4	solid	2.1595E-04 (0.05 g)
H_2SO_4	aqueous	0.035
N_2H_4	aqueous	0.050
$CuSO_4$	solid	5.0E-04–1.0E-01
H_2O	aqueous	55.5082 (1 L)
Temperature		95 °C
Pressure		1 bar

Table 2
Results of equilibrium calculations using the aqueous model of the HSC Chemistry® 9 for the HyBRID dissolution of magnetite at the raw amount of $CuSO_4$ of 5.0E-04 mol.

Data Type	Species or ion	Phase	Unit	Temperature [°C]							
				25	35	45	55	65	75	85	95
Raw Amount	H_2O	aqueous	mol	55.5082	55.5082	55.5082	55.5082	55.5082	55.5082	55.5082	55.5082
	H_2SO_4(l)	aqueous	mol	0.035	0.035	0.035	0.035	0.035	0.035	0.035	0.035
	N_2H_4(l)	aqueous	mol	0.050	0.050	0.050	0.050	0.050	0.050	0.050	0.050
	Fe_3O_4(s)	pure solid	mol	2.1595E-04	2.1595E-04	2.1595E-04	2.1595E-04	2.1595E-04	2.1595E-04	2.1595E-04	2.1595E-04
	$CuSO_4$(s)	pure solid	mol	5.0E-04	5.0E-04	5.0E-04	5.0E-04	5.0E-04	5.0E-04	5.0E-04	5.0E-04
Equilibrium Amount	N_2(g)	gas	mol	2.330E-04	2.330E-04	2.330E-04	2.330E-04	2.330E-04	2.330E-04	2.330E-04	2.330E-04
	H_2O	aqueous	mol	55.5091	55.5091	55.5091	55.5091	55.5091	55.5091	55.5091	55.5091
	H_2SO_4(l)	aqueous	mol	1.008E-14	2.694E-14	6.642E-14	1.512E-13	3.192E-13	6.274E-13	1.154E-12	2.000E-12
	N_2H_4(l)	aqueous	mol	4.757E-10	1.148E-09	2.705E-09	6.253E-09	1.422E-08	3.188E-08	7.057E-08	1.544E-07
	$N_2H_5^+$	aqueous	mol	4.977E-02	4.977E-02	4.977E-02	4.977E-02	4.977E-02	4.977E-02	4.977E-02	4.977E-02
	Fe^{3+}	aqueous	mol	5.330E-20	7.636E-20	1.030E-19	1.314E-19	1.591E-19	1.835E-19	2.023E-19	2.141E-19
	Fe^{2+}	aqueous	mol	6.479E-04	6.479E-04	6.479E-04	6.479E-04	6.479E-04	6.479E-04	6.479E-04	6.479E-04
	Cu^{2+}	aqueous	mol	4.744E-12	3.721E-12	2.841E-12	2.114E-12	1.536E-12	1.092E-12	7.607E-13	5.210E-13
	Cu^+	aqueous	mol	5.000E-04	5.000E-04	5.000E-04	5.000E-04	5.000E-04	5.000E-04	5.000E-04	5.000E-04
	H^+	aqueous	mol	1.123E-02	9.978E-03	8.683E-03	7.400E-03	6.181E-03	5.064E-03	4.075E-03	3.226E-03
	OH^-	aqueous	mol	1.594E-12	3.686E-12	8.126E-12	1.722E-11	3.529E-11	7.030E-11	1.366E-10	2.595E-10
	SO_4^{2-}	aqueous	mol	2.729E-02	2.604E-02	2.475E-02	2.346E-02	2.224E-02	2.113E-02	2.014E-02	1.929E-02
	HSO_4^-	aqueous	mol	8.212E-03	9.459E-03	1.075E-02	1.204E-02	1.326E-02	1.437E-02	1.536E-02	1.621E-02
	Fe_3O_4(s)	pure solid	mol	0.000E+00	0.000E+00	0.000E+00	0.000E+00	0.000E+00	0.000E+00	0.000E+00	0.000E+00
	Fe_2O_3(s)	pure solid	mol	0.000E+00	0.000E+00	0.000E+00	0.000E+00	0.000E+00	0.000E+00	0.000E+00	0.000E+00
	$CuSO_4$(s)	pure solid	mol	0.000E+00	0.000E+00	0.000E+00	0.000E+00	0.000E+00	0.000E+00	0.000E+00	0.000E+00
	Cu_2O(s)	pure solid	mol	0.000E+00	0.000E+00	0.000E+00	0.000E+00	0.000E+00	0.000E+00	0.000E+00	0.000E+00
	$Cu(OH)_2$(s)	pure solid	mol	0.000E+00	0.000E+00	0.000E+00	0.000E+00	0.000E+00	0.000E+00	0.000E+00	0.000E+00
Activity coefficient	N_2(g)	gas	–	1.0000	1.0000	1.0000	1.0000	1.0000	1.0000	1.0000	1.0000
	H_2O	aqueous	–	1.0003	1.0003	1.0003	1.0003	1.0003	1.0003	1.0003	1.0003
	H_2SO_4(l)	aqueous	–	1.0018	1.0017	1.0017	1.0017	1.0017	1.0016	1.0016	1.0016
	N_2H_4(l)	aqueous	–	1.0018	1.0017	1.0017	1.0017	1.0017	1.0016	1.0016	1.0016
	$N_2H_5^+$	aqueous	–	0.7521	0.7508	0.7494	0.7477	0.7458	0.7434	0.7405	0.7371
	Fe^{3+}	aqueous	–	0.0759	0.0747	0.0735	0.0721	0.0704	0.0684	0.0661	0.0634
	Fe^{2+}	aqueous	–	0.2823	0.2827	0.2833	0.2836	0.2834	0.2824	0.2804	0.2773
	Cu^{2+}	aqueous	–	0.2594	0.2532	0.2475	0.2421	0.2367	0.2311	0.2250	0.2183
	Cu^+	aqueous	–	0.7521	0.7508	0.7494	0.7477	0.7458	0.7434	0.7405	0.7371
	H^+	aqueous	–	0.7623	0.7613	0.7603	0.7591	0.7576	0.7556	0.7531	0.7500
	OH^-	aqueous	–	0.7516	0.7503	0.7489	0.7473	0.7453	0.7430	0.7402	0.7367
	SO_4^{2-}	aqueous	–	0.3148	0.3120	0.3091	0.3059	0.3022	0.2979	0.2928	0.2870
	HSO_4^-	aqueous	–	0.7406	0.7398	0.7387	0.7372	0.7352	0.7327	0.7296	0.7258
	Fe_3O_4(s)	pure solid	–	1.0000	1.0000	1.0000	1.0000	1.0000	1.0000	1.0000	1.0000
	Fe_2O_3(s)	pure solid	–	1.0000	1.0000	1.0000	1.0000	1.0000	1.0000	1.0000	1.0000
	$CuSO_4$(s)	pure solid	–	1.0000	1.0000	1.0000	1.0000	1.0000	1.0000	1.0000	1.0000
	Cu_2O(s)	pure solid	–	1.0000	1.0000	1.0000	1.0000	1.0000	1.0000	1.0000	1.0000
	$Cu(OH)_2$(s)	pure solid	–	1.0000	1.0000	1.0000	1.0000	1.0000	1.0000	1.0000	1.0000
pH of solution				2.067	2.119	2.180	2.250	2.329	2.417	2.513	2.616

the other hand, in the case of a larger amount of raw $CuSO_4$ (5.0E-02 mol), considerable amounts of Cu_2O precipitated were observed. The amount of Cu_2O precipitate produced slightly decreased with increasing temperature. Regardless of whether the raw (input) amount of $CuSO_4$ was small or large, no generation of $Cu(OH)_2$ solid precipitate was found. Although not shown in this paper, the HyBRID decontamination experiments conducted at the KAERI laboratory have also shown the formation of Cu_2O precipitates at large amounts of raw $CuSO_4$ fed. Therefore, the calculation results performed in this study showing the production of Cu_2O precipitates can be considered to be in agreement with the experimental results.

Fig. 2 shows the effect of the raw amount of $CuSO_4$ on the equilibrium amounts of key species and ions as a function of temperature in the HyBRID dissolution of magnetite. In particular, attention should be paid to the equilibrium amount of Cu_2O solid precipitated (solid lines in figures). In all cases, no $Cu(OH)_2$ precipitates was produced at all. At very low amounts of raw $CuSO_4$ (5.0E-04 mol and 1.0E-03 mol), no precipitation of Cu_2O occurred. However, the production of Cu_2O precipitates occurred when the raw amount of $CuSO_4$ was 5.0E-03 mol, as seen in Fig. 2(c). The amount of Cu_2O produced increased with the increase of the raw amount of $CuSO_4$ and decreased with the increase of the temperature. Not surprisingly, the equilibrium amounts of copper ions (Cu^+ and Cu^{2+}) increased with increasing the raw amount of $CuSO_4$. The equilibrium amounts of the Fe^{2+} ion were almost constant regardless of the raw amount of $CuSO_4$ and the temperature.

The effect of the raw amount of $CuSO_4$ and temperature on the amount of Cu_2O precipitates produced in the HyBRID dissolution of magnetite is more distinctly shown in Figs. 3 and 4. From the graphs in Fig. 2, only the data on the amount of Cu_2O precipitates were taken and combined, and shown in Fig. 3 for ease of viewing. At all temperatures, the amount of Cu_2O at equilibrium increased significantly as the amount of raw $CuSO_4$ added to the solution increased. Fig. 4 shows the amount of Cu_2O precipitates at equilibrium as a function of the raw amount of $CuSO_4$ at three different temperatures. As the raw amount of $CuSO_4$ increased and the temperature decreased, the amount of Cu_2O produced increased.

Fig. 5 shows the change in the pH of the aqueous solution as a function of temperature at various amounts of raw $CuSO_4$ introduced. At all the raw amounts of $CuSO_4$, the calculated pH values of the solution gradually increased with increasing temperature. The change in the pH values of the solution as a function of the raw amount of $CuSO_4$ at three representative temperatures is shown in Fig. 6. In regions where the raw amount of $CuSO_4$ was very small, the pH decreased slightly as the raw amount of $CuSO_4$ increased. However, as the raw amount of $CuSO_4$ was further increased, the pH

Table 3
Results of equilibrium calculations using the aqueous model of the HSC Chemistry® 9 for the HyBRID dissolution of magnetite at the raw amount of $CuSO_4$ of 5.0E-02 mol.

Data Type	Species or ion	Phase	Unit	Temperature [°C]							
				25	35	45	55	65	75	85	95
Raw Amount	H_2O	aqueous	mol	55.5082	55.5082	55.5082	55.5082	55.5082	55.5082	55.5082	55.5082
	H_2SO_4(l)	aqueous	mol	0.035	0.035	0.035	0.035	0.035	0.035	0.035	0.035
	N_2H_4(l)	aqueous	mol	0.050	0.050	0.050	0.050	0.050	0.050	0.050	0.050
	Fe_3O_4(s)	pure solid	mol	2.1595E-04	2.1595E-04	2.1595E-04	2.1595E-04	2.1595E-04	2.1595E-04	2.1595E-04	2.1595E-04
	$CuSO_4$(s)	pure solid	mol	5.0E-02	5.0E-02	5.0E-02	5.0E-02	5.0E-02	5.0E-02	5.0E-02	5.0E-02
Equilibrium Amount	N_2(g)	gas	mol	1.261E-02	1.261E-02	1.261E-02	1.261E-02	1.261E-02	1.261E-02	1.261E-02	1.261E-02
	H_2O	aqueous	mol	55.4885	55.4890	55.4895	55.4901	55.4906	55.4912	55.4918	55.4924
	H_2SO_4(l)	aqueous	mol	3.796E-13	1.009E-12	2.517E-12	5.926E-12	1.324E-11	2.821E-11	5.761E-11	1.133E-10
	N_2H_4(l)	aqueous	mol	5.307E-11	1.234E-10	2.759E-10	5.940E-10	1.234E-09	2.478E-09	4.819E-09	9.100E-09
	$N_2H_5^+$	aqueous	mol	3.739E-02	3.739E-02	3.739E-02	3.739E-02	3.739E-02	3.739E-02	3.739E-02	3.739E-02
	Fe^{3+}	aqueous	mol	1.101E-18	1.655E-18	2.395E-18	3.356E-18	4.578E-18	6.102E-18	7.970E-18	1.022E-17
	Fe^{2+}	aqueous	mol	6.479E-04	6.479E-04	6.479E-04	6.479E-04	6.479E-04	6.479E-04	6.479E-04	6.479E-04
	Cu^{2+}	aqueous	mol	8.995E-10	7.918E-10	6.846E-10	5.854E-10	4.979E-10	4.232E-10	3.605E-10	3.082E-10
	Cu^+	aqueous	mol	8.922E-03	9.934E-03	1.096E-02	1.202E-02	1.311E-02	1.426E-02	1.545E-02	1.671E-02
	H^+	aqueous	mol	7.251E-02	6.670E-02	6.106E-02	5.576E-02	5.089E-02	4.649E-02	4.253E-02	3.899E-02
	OH^-	aqueous	mol	2.712E-13	5.995E-13	1.243E-12	2.435E-12	4.529E-12	8.037E-12	1.366E-11	2.232E-11
	SO_4^{2-}	aqueous	mol	3.512E-02	3.032E-02	2.571E-02	2.147E-02	1.769E-02	1.443E-02	1.167E-02	9.388E-03
	HSO_4^-	aqueous	mol	4.988E-02	5.468E-02	5.929E-02	6.353E-02	6.731E-02	7.057E-02	7.333E-02	7.561E-02
	Fe_3O_4(s)	pure solid	mol	0.000E+00	0.000E+00	0.000E+00	0.000E+00	0.000E+00	0.000E+00	0.000E+00	0.000E+00
	Fe_2O_3(s)	pure solid	mol	0.000E+00	0.000E+00	0.000E+00	0.000E+00	0.000E+00	0.000E+00	0.000E+00	0.000E+00
	$CuSO_4$(s)	pure solid	mol	0.000E+00	0.000E+00	0.000E+00	0.000E+00	0.000E+00	0.000E+00	0.000E+00	0.000E+00
	Cu_2O(s)	pure solid	mol	2.054E-02	2.003E-02	1.952E-02	1.899E-02	1.844E-02	1.787E-02	1.727E-02	1.664E-02
	$Cu(OH)_2$(s)	pure solid	mol	0.000E+00	0.000E+00	0.000E+00	0.000E+00	0.000E+00	0.000E+00	0.000E+00	0.000E+00
Activity coefficient	N_2(g)	gas	–	1.0000	1.0000	1.0000	1.0000	1.0000	1.0000	1.0000	1.0000
	H_2O	aqueous	–	1.0005	1.0005	1.0005	1.0004	1.0004	1.0004	1.0004	1.0004
	H_2SO_4(l)	aqueous	–	1.0037	1.0036	1.0035	1.0034	1.0034	1.0033	1.0033	1.0032
	N_2H_4(l)	aqueous	–	1.0037	1.0036	1.0035	1.0034	1.0034	1.0033	1.0033	1.0032
	$N_2H_5^+$	aqueous	–	0.7033	0.7050	0.7064	0.7075	0.7079	0.7076	0.7064	0.7044
	Fe^{3+}	aqueous	–	0.0409	0.0418	0.0426	0.0432	0.0435	0.0433	0.0427	0.0416
	Fe^{2+}	aqueous	–	0.2886	0.2996	0.3112	0.3226	0.3329	0.3416	0.3479	0.3517
	Cu^{2+}	aqueous	–	0.2483	0.2538	0.2604	0.2676	0.2748	0.2814	0.2869	0.2910
	Cu^+	aqueous	–	0.7033	0.7050	0.7064	0.7075	0.7079	0.7076	0.7064	0.7044
	H^+	aqueous	–	0.7431	0.7469	0.7506	0.7537	0.7560	0.7571	0.7571	0.7558
	OH^-	aqueous	–	0.7027	0.7044	0.7060	0.7071	0.7076	0.7073	0.7062	0.7042
	SO_4^{2-}	aqueous	–	0.2335	0.2344	0.2351	0.2352	0.2344	0.2327	0.2300	0.2261
	HSO_4^-	aqueous	–	0.7318	0.7330	0.7338	0.7338	0.7331	0.7316	0.7291	0.7258
	Fe_3O_4(s)	pure solid	–	1.0000	1.0000	1.0000	1.0000	1.0000	1.0000	1.0000	1.0000
	Fe_2O_3(s)	pure solid	–	1.0000	1.0000	1.0000	1.0000	1.0000	1.0000	1.0000	1.0000
	$CuSO_4$(s)	pure solid	–	1.0000	1.0000	1.0000	1.0000	1.0000	1.0000	1.0000	1.0000
	Cu_2O(s)	pure solid	–	1.0000	1.0000	1.0000	1.0000	1.0000	1.0000	1.0000	1.0000
	$Cu(OH)_2$(s)	pure solid	–	1.0000	1.0000	1.0000	1.0000	1.0000	1.0000	1.0000	1.0000
pH of solution				1.268	1.302	1.338	1.376	1.414	1.453	1.492	1.530

values were markedly reduced.

Fig. 7 shows the E-pH diagrams for Cu constructed at a constant temperature of 95 °C and at various concentrations of Cu. The temperature of 95 °C is actually the condition of the HyBRID decontamination experiments conducted at KAERI. It gives the pH values at the boundaries between the region where Cu exists in the form of Cu^+ ion and the region where Cu exists in the form of Cu_2O solid. The pH boundaries between the Cu^{2+} region and the $Cu(OH)_2$ solid region are also shown. The pH values varied depending on the total concentration of Cu. As the Cu concentration increased, the pH boundaries shifted to the left. As shown in Fig. 7, the pathway for the formation of $Cu(OH)_2$ from Cu^+ is as follows. As the redox potential of the solution increases, Cu^+ ions are oxidized to Cu^{2+} ions. Then the Cu^{2+} ions are hydrolyzed to $Cu(OH)_2$ as the pH of the solution increases. Therefore, at a higher redox potential and pH of the solution, the $Cu(OH)_2$ precipitates instead of Cu(OH) can be formed. At lower redox potentials, as the pH of the solution increases, Cu^+ ions are converted to Cu_2O(s) precipitates instead of being hydrolyzed to $Cu(OH)_2$ or Cu(OH). According to the equilibrium calculations given in Fig. 2, there was no precipitation of both $Cu(OH)_2$ and CuOH under the reducing conditions of this study.

Fig. 8 illustrates the relationship between the pH value and the Cu concentration at two boundaries between stability areas at 95 °C. The pH value decreased linearly with increasing the logarithm of the Cu concentration. Since the species affecting the magnetite dissolution is Cu^+ ions, it is important to adjust so that the Cu^+ ions do not change to Cu^{2+}, Cu_2O(s), or $Cu(OH)_2$(s). To prevent the Cu^+ ions from being oxidized to the Cu^{2+} ions, the redox potential should be lower than 0.2 V by adding N_2H_4. According to the HyBRID experiments conducted at KAERI, no $Cu(OH)_2$ precipitates was observed since the redox potential was kept neutral (0.0 V). Moreover, in order to prevent the formation of Cu_2O precipitates from Cu^+ ions, the pH of the solution should be made as low as possible, depending on the Cu concentration.

Table 4 shows the equilibrium amounts of Cu_2O and $Cu(OH)_2$ and the pH values of the solution calculated for various amounts of raw $CuSO_4$ at 95 °C. It also gives the pH values at the boundaries between the stability areas of Cu^+ and Cu_2O obtained from the E-pH diagrams for Cu (Fig. 7) at corresponding Cu concentrations. As already mentioned earlier, precipitation of $Cu(OH)_2$ did not occur at any $CuSO_4$ amounts and the solution pH decreased with the increase of the raw amount of $CuSO_4$. When the raw amount of $CuSO_4$ was 1.0E-03 or less, there was no precipitation of Cu_2O because the solution pH was lower than the pH value obtained from the E-pH diagram, indicating that the solution was in a region where only Cu^+ ions were stably present. Interestingly, when the raw amount of $CuSO_4$ was 1.0E-03, the pH value of the solution obtained from the equilibrium calculation exactly matched the pH value obtained from the E-pH

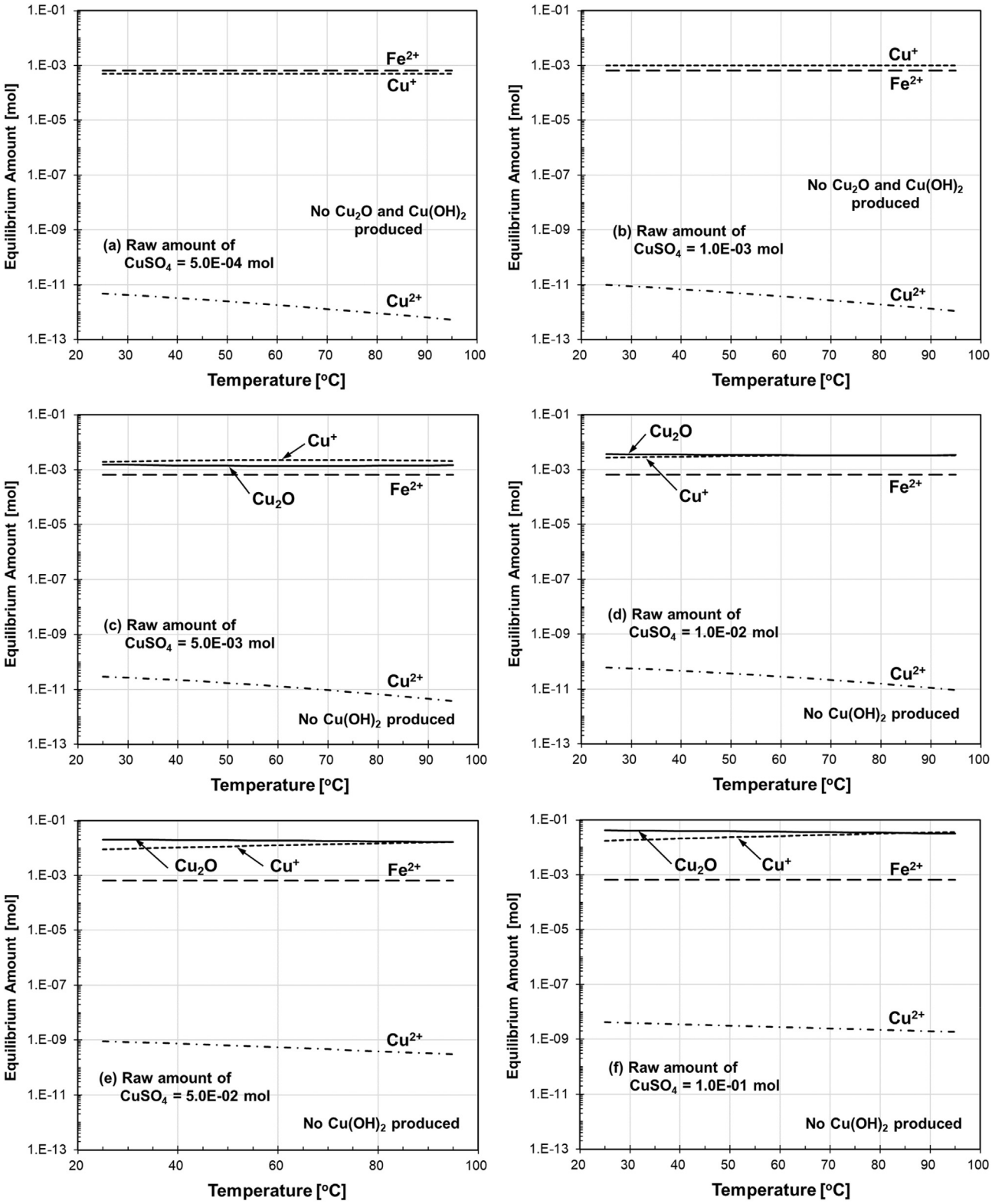

Fig. 2. Effect of raw amount of $CuSO_4$ on the equilibrium amounts of key species and ions (pay particular attention to Cu_2O: solid lines) as a function of temperature in the HyBRID dissolution of magnetite. Raw amount of $CuSO_4$ in mole is given inside each figure. The raw amounts of other species except $CuSO_4$ are kept constant, as given in Table 1. The equilibrium amounts of Fe^{3+} are negligibly small and are not included in the figures.

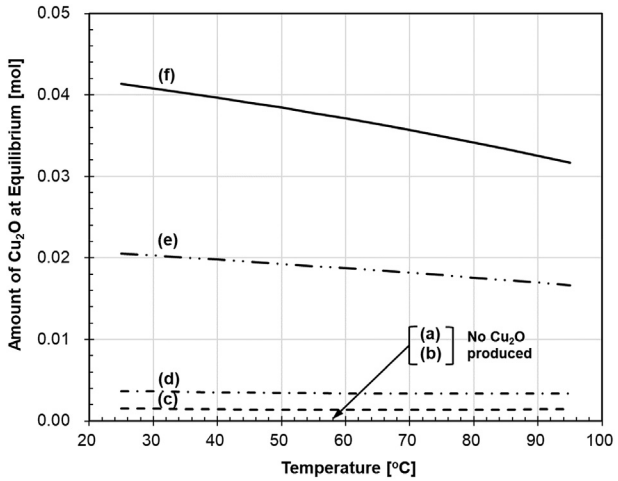

Fig. 3. Equilibrium amount of Cu_2O(s) calculated at different raw amounts of $CuSO_4$ in the HyBRID dissolution of magnetite. Raw amount of $CuSO_4$ in mole: (a) 5.0E-04; (b) 1.0E-03; (c) 5.0E-03; (d) 1.0E-02; (e) 5.0E-02; (f) 1.0E-01. The raw amounts of other species except $CuSO_4$ are given in Table 1.

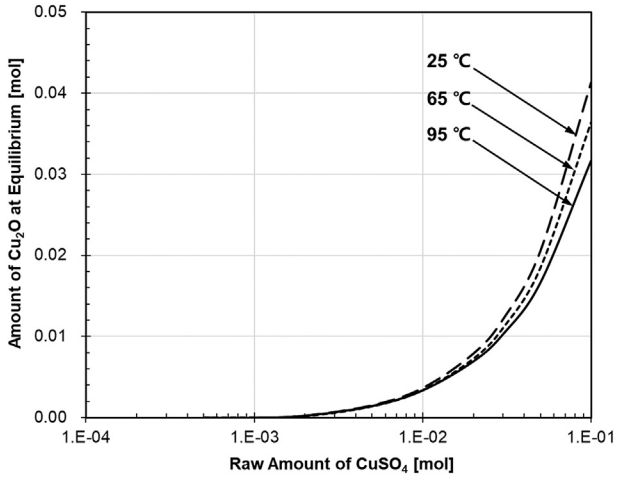

Fig. 4. Equilibrium amounts of Cu_2O(s) as a function of the raw amount of $CuSO_4$ calculated at three different temperatures in the HyBRID dissolution of magnetite. The raw amounts of other species except $CuSO_4$ are given in Table 1.

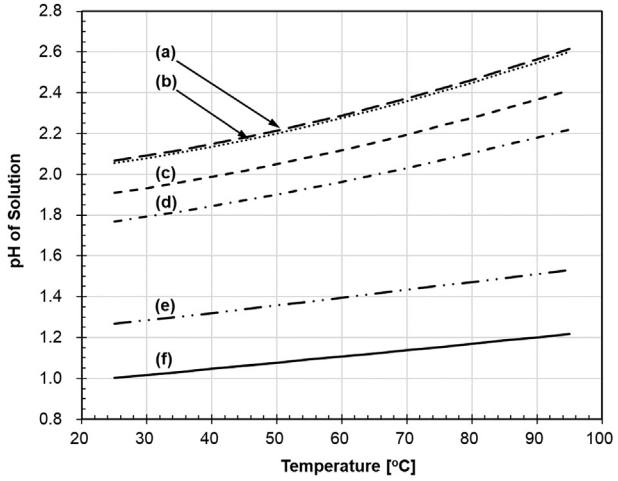

Fig. 5. pH of solution as a function of temperature calculated at different raw amounts of $CuSO_4$ in the HyBRID dissolution of magnetite. Raw amount of $CuSO_4$ in mole: (a) 5.0E-04; (b) 1.0E-03; (c) 5.0E-03; (d) 1.0E-02; (e) 5.0E-02; (f) 1.0E-01. The raw amounts of other species except $CuSO_4$ are given in Table 1.

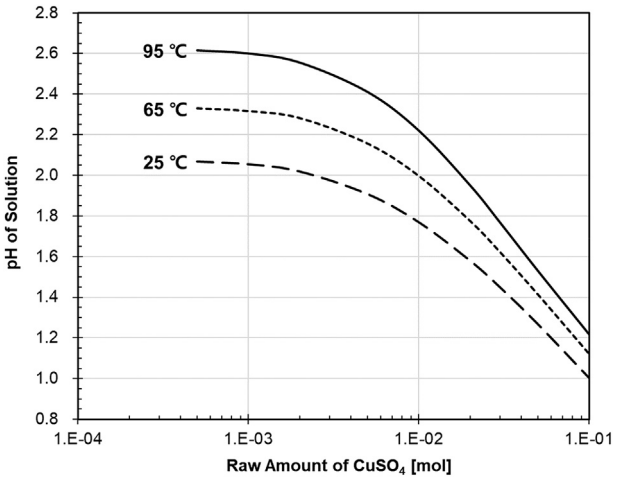

Fig. 6. pH of solution as a function of the raw amount of $CuSO_4$ calculated at three different temperatures in the HyBRID dissolution of magnetite. The raw amounts of other species except $CuSO_4$ are given in Table 1.

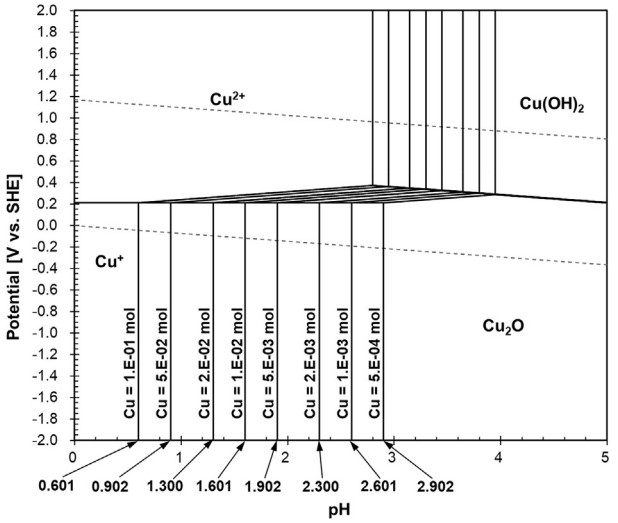

Fig. 7. E-pH diagrams for Cu at 95 °C.

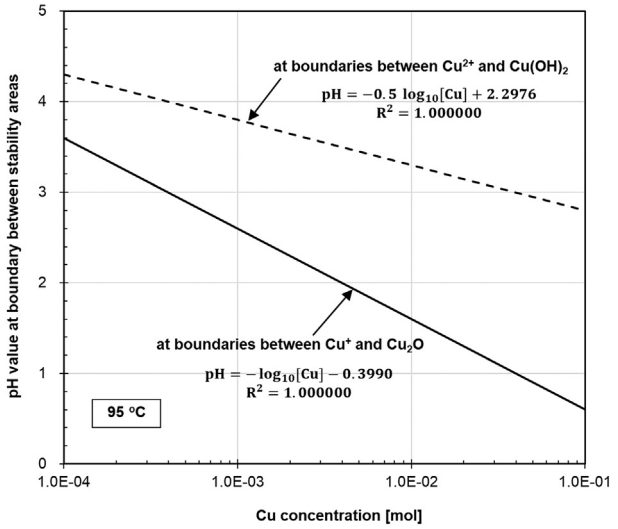

Fig. 8. The pH values at the boundaries between stability areas as a function of Cu concentration at 95 °C.

Table 4
Comparison of the results of equilibrium calculations conducted by using the recipe of Table 1 and the results of E-pH diagram at 95 °C.

Raw amount of $CuSO_4$ [mol]	At equilibrium			pH at boundary between Cu^+ and Cu_2O in E-pH diagram
	Amount of Cu_2O [mol]	Amount of $Cu(OH)_2$ [mol]	pH of solution	
5.0E-04	0.0000	0.0000	2.616	2.902
1.0E-03	0.0000	0.0000	2.601	2.601
2.0E-03	0.0002	0.0000	2.556	2.300
5.0E-03	0.0015	0.0000	2.411	1.902
1.0E-02	0.0034	0.0000	2.221	1.601
2.0E-02	0.0070	0.0000	1.951	1.300
5.0E-02	0.0166	0.0000	1.530	0.902
1.0E-01	0.0317	0.0000	1.217	0.601

diagram. However, when the raw amount of $CuSO_4$ was 2.0E-03 or more, the pH value of the solution from the equilibrium calculation was higher than that from the E-pH diagram, causing the precipitation of Cu_2O. In addition, the greater the difference between the pH value from the equilibrium calculation and the pH value from the E-pH diagram, the greater the amount of Cu_2O produced. Consequently, the results of this study provide guidelines for the input amounts of the raw materials, especially $CuSO_4$, and the pH values of the solution, which prevent Cu^+ ions from converting to Cu_2O precipitates in the HyBRID dissolution experiments for magnetite.

4. Conclusions

The reaction mechanisms of acidic and reductive dissolution of magnetite using the HyBRID decontamination method were proposed. The chemical equilibrium of the HyBRID aqueous system for magnetite (Fe_3O_4–$CuSO_4$–N_2H_4–H_2SO_4–H_2O) was calculated at various temperatures from 25 °C to 95 °C and at 1 bar by using the HSC Chemistry® 9 software. The recipe of raw materials fed is based on the experiments actually conducted at KAERI. In particular, this work is focused on the effect of the raw amount of $CuSO_4$ on the formation of Cu_2O or $Cu(OH)_2$ precipitates. The equilibrium amount of the Fe^{3+} ion was almost negligible at all temperatures, which can be attributed to the reduction of Fe^{3+} ions to Fe^{2+} ions by N_2H_4. Similarly, the equilibrium amount of Cu^{2+} was negligibly small due to the reduction of Cu^{2+} to Cu^+ by the reaction with $N_2H_5^+$. Almost all of N_2H_4 was protonated to produce $N_2H_5^+$ ions. As the raw amount of $CuSO_4$ added increased, the production of Cu_2O precipitates occurred. The amount of Cu_2O produced increased with increasing the raw amount of $CuSO_4$ and slightly decreased with increasing the temperature. Regardless of how much $CuSO_4$ was added, no $Cu(OH)_2$ precipitate was produced at all. The calculated pH values of the aqueous solution gradually increased with increasing temperature and significantly decreased with increasing the raw amount of $CuSO_4$.

The E-pH diagrams for Cu constructed at various concentrations of Cu provided the effect of the Cu concentration on the pH values at boundaries where the coexistence of Cu^+ ion and Cu_2O solid occurred. The pH value decreased linearly with increasing the logarithm of the Cu concentration. To ensure that Cu^+ ions are not oxidized to Cu^{2+} ions and $Cu(OH)_2$ is not produced, the redox potential of the solution should be kept below 0.2 V. To prevent Cu^+ ions from being precipitated to $Cu_2O(s)$, the raw amount of $CuSO_4$ should be adjusted so that the pH value of the aqueous solution obtained from the equilibrium calculation is less than that found from the E-pH diagram. For the recipe of the HyBRID experiments considered in this work, the raw amount of $CuSO_4$ must be 1.0E-03 mol or less.

Acknowledgments

This work has been carried out under the Nuclear R&D Program (NRF-2018M2A8A5024102 & NRF-2017M2A8 A5015144f) funded by Ministry of Science and ICT.

Appendix A. Supplementary data

Supplementary data to this article can be found online at https://doi.org/10.1016/j.net.2020.04.012.

References

[1] J.K. Moon, S.B. Kim, W.K. Choi, B.S. Choi, D.Y. Chung, B.K. Seo, The status and prospect of decommissioning technology development at KAERI, J. Nucl. Fuel Cycle Waste Technol. 17 (2019) 139–165.
[2] Technical Report Series No, 395, State of the Art Technology for Decontamination and Dismantling of Nuclear Facilities, IAEA, Vienna, 1999.
[3] Technical Report Series No, 386, Decommissioning of Nuclear Facilities Other than Reactors, IAEA, Vienna, 1998.
[4] H.J. Won, W.S. Lee, C.H. Jung, S.Y. Park, W.K. Choi, J.K. Moon, A feasibility study on the decontamination of type 304 stainless steel by N_2H_4 base solution, Asian J. Chem. 26 (2014) 1327–1330.
[5] J.Y. Jung, S.Y. Park, H.J. Won, S.B. Kim, W.K. Choi, J.K. Moon, S.J. Park, Corrosion properties of inconel-600 and 304 stainless steel in new oxidative and reductive decontamination reagent, Met. Mater. Int. 21 (2015) 678–685.
[6] W.K. Choi, Development of Advanced Decontamination Technology for Nuclear Facilities, KAERI, 2017. Report No. 2012M2A8A5025655.
[7] W.K. Choi, H.J. Won, S.Y. Park, S.B. Kim, J.Y. Jung, J.K. Moon, Chemical decommissioning of a primary coolant system using hydrazine-based solutions, in: Waste Management Conference, Proceedings, Paper No 15215, Phoenix, Arizona, USA, March 15-19, 2015.
[8] H.J. Won, W.S. Lee, C.H. Jung, S.Y. Park, W.K. Choi, J.K. Moon, Dissolution of Fe_3O_4 by the N_2H_4 base solution, in: 7th International Conference on Multifunctional Materials and Applications, Proceedings, Huainan, China, Nov., vols. 22–23, 2013.
[9] B.-C. Lee, S.-B. Kim, J.-K. Moon, S.-Y. Park, Evaluation of reaction spontaneity for acidic and reductive dissolutions of corrosion metal oxides using HyBRID chemical decontamination, J. Radioanal. Nucl. Chem. 323 (2020) 91–103.
[10] S.-B. Kim, S.-Y. Park, W.-K. Choi, H.-J. Won, J.-S. Park, B.-K. Seo, Magnetite dissolution by copper catalyzed reductive decontamination, J. Nucl. Fuel Cycle Waste Technol. 16 (2018) 421–429.
[11] K.S. Pitzer, Thermodynamics of electrolytes. I. Theoretical basis and general equations, J. Phys. Chem. 77 (1973) 268–277.
[12] C.E. Harvie, J.H. Weare, The prediction of mineral solubilities in natural waters: the Na-K-Mg-Ca-Cl-SO_4-H_2O system from zero to high concentration at 25°C, Geochem. Cosmochim. Acta 44 (1980) 981–997.
[13] C.E. Harvie, N. Møller, J.H. Weare, The prediction of mineral solubilities in natural waters: the Na-K-Mg-Ca-H-Cl-SO_4-OH-HCO_3-CO_3-CO_2-H_2O system to high ionic strengths at 25°C, Geochem. Cosmochim. Acta 48 (1984) 723–751.
[14] K.S. Pitzer, Thermodynamics, third ed., McGraw-Hill, 1995.
[15] K.S. Pitzer, Activity Coefficients in Electrolyte Solutions, CRC Press, 1979.
[16] J.M. Prausnitz, R.N. Lichtenthaler, E. Gomes de Azevedo, Molecular Thermodynamics of Fluid- Phase Equilibria, third ed., Prentice-Hall, 1999.
[17] J.F. Zemaitis Jr., D.M. Clark, M. Rafal, N.C. Scrivner, Handbook of Aqueous Electrolyte Thermodynamics, Wiley-Interscience, 1986.
[18] HSC Chemistry software. www.outotec.com.
[19] H. Haung, Construction of Eh–pH and other stability diagrams of uranium in a multicomponent system with a microcomputer–I. Domains of predominance diagrams, Canadian Metallurgical Quarterly 28 (1989) 225–239.